Available online at www.sciencedirect.com

ScienceDirect

Ceramics International 35 (2009) 1725–1729

CERAMICS INTERNATIONAL

www.elsevier.com/locate/ceramint

The effects of incomplete combustion on $Ba_2Ti_9O_{20}$ phase formation in a citrate solution combustion method

Xiao Lou, Wenjian Weng [*], Kui Cheng, Chenlu Song,
Piyi Du, Ge Shen, Gaorong Han

Department of Materials Science & Engineering, Zhejiang University, Hangzhou 310027, China

Received 7 May 2008; received in revised form 23 May 2008; accepted 29 September 2008
Available online 22 October 2008

Abstract

In this work, pure $Ba_2Ti_9O_{20}$ (B_2T_9) ceramics phases are prepared at 1300 °C after precursor solution combustion, powders calcination and sintering. The effects of incomplete combustion on B_2T_9 formation during the citrate solution combustion (CSC) process were studied. Different precursor solutions were designed and prepared to control the completeness of combustion. The results showed complete combustion product facilitates B_2T_9 formation; while incomplete combustion product, which is an inhomogeneous Ti-rich amorphous phase, affects the intermediate phase formation after calcining, and finally inhibits B_2T_9 formation.

Keywords: Calcination; Sintering; Citrate solution combustion

1. Introduction

Over the past decades, the BaO–TiO_2 system has attracted much attention due to their excellent microwave dielectric performances in the application of resonators and capacitors [1–4]. Conventionally, BaO–TiO_2 system materials were prepared by the solid-state reaction method [3], which, however, always exhibited poor controls on powder stoichiometry, powder size and its distribution [5,6]. Recently, wet chemical methods for preparing BaO–TiO_2 ceramic powders become increasingly significant because of the easiness in acquiring homogeneous, ultra fine, high-purity and stoichiometric ceramic powders [7–11].

As a special wet chemical method, solution-combustion (SC) has many advantages. In SC process, nitrate ions usually act as oxidant, while organics, such as urea [12], carbohydrazide [13], oxalic dihydrazide [14], citric acid [15], glycine [16] etc., provide the "fuel" for combustion.

Among all these organics, citric acid (CA) is reported to be effective in such process because of its good chelating ability and flammability. A series of multicomponent oxides have been prepared through the citrate solution combustion (CSC) routes [15–18].

Owing to the incomplete oxidation of CA in the CSC process, however, the residual organic component in the as-combusted powder is inevitable, which was reported to be an inhibitor of the crystallization [19–21]. Although the reason is roughly ascribed to carbon thermic reduction and some other effects [22–23], the exact reason of incomplete combustion inhibiting the formation of crystalline multicomponent oxide phase is still unclear.

In this work, $Ba_2Ti_9O_{20}$ (B_2T_9), which is known as superior dielectric ceramics, was synthesized by the CSC route in the $TiO(NO_3)_2$–$Ba(NO_3)_2$–$C_6H_8O_7{\cdot}H_2O$(CA)–NH_4NO_3(AN) system. Since B_2T_9 phase formation is sensitive to preparation conditions [15,19,20,24], it is suitably selected to study the effect of the combustion process on the phase formation. Different precursor solutions were designed and prepared by adding corresponding oxidants to control the completeness of combustion, and to find how the incomplete combustion and organic residuals influence the phase formation.

2. Experimental procedure

$Ti(OC_2H_5)_4$, $Ba(NO_3)_2$, citric acid and NH_4NO_3 (AN) were selected as raw materials, all of which were analytically pure.

---

[*] Corresponding author. Tel.: +86 571 87953787; fax: +86 571 87953787.
E-mail address: wengwj@zju.edu.cn (W. Weng).

doi:10.1016/j.ceramint.2008.09.013

Table 1
Composition of starting precursors.

Sample no.	Ba:Ti:CA:AN (2:9:12:X)
X1	2:9:12:0
X2	2:9:12:53
X3	2:9:12:106

Citric acid (CA) was used as the complexing reagent and the fuel as well. $Ti(OC_2H_5)_4$ was first dissolved in nitric acid solution to become a titanyl nitrate ($TiO(NO_3)_2$) solution as described by Xu et al. [8]. The ready-to-combust solutions were then prepared through dissolving barium nitrate and citrate acid in the titanyl nitrate solution in a Ba:Ti:CA molar ratio of 2:9:12. During the preparation of the solution, the pH value was maintained at 6 through addition of aqueous ammonia. To study the influence of combustion completeness, a series of mixed solutions with different amount of NH_4NO_3 (AN) were prepared, and are tabulated in Table 1. The citrate complex solutions were heated on a hot plate until combusted spontaneously. After the burnt powders were calcined at 900 °C for 4 h, they were pressed into small discs with 15 mm in diameter at a pressure of 100 MPa. The discs were finally sintered at 1300 °C for 4 h to become ceramics.

The phases of the samples after burning, calcining and singtering were subsequently identified through X-ray powder diffractometer with Cu Kα (XRD, D/MAX-rA). The chemical groups and bondings in the burnt powders were determined by Fourier transform infrared spectroscopy (FT-IR, Nicolet-Avatar 360). The chemical elements of the combusted powders were characterized by the element analyzer (Flash EA 1112, made by ThermoFinnigan). The morphology of the burnt powders was observed under transmission electron microscopy (TEM, Model JEM-100CX, JEOL Co.), during which the chemical elements in the local areas were analyzed using EDAX attached to the TEM.

3. Results

FT-IR spectra of burnt products are shown in Fig. 1. A broad band is observed at 500–700 cm^{-1} corresponding to a Ti–O stretching mode, and the bands at 2790 cm^{-1} and 1050 cm^{-1} are attributed to C–H and C–O bonding, respectively. The intensities of both C–H band and C–O band gradually decrease with increasing amount of NH_4NO_3 from sample X1 to X3, which indicates less residual organic components. The element analysis of the burnt products is tabulated in Table 2: carbon contents are 4.481wt%, 1.512 wt % and 1.159 wt % in X1, X2, X3, respectively, again showing that the carbon content decreases with adding NH_4NO_3. Fig. 2 shows the XRD patterns of the burnt product samples. The main phase of powders is $BaTi_4O_9$ (BT_4, JCPDS 34-0070) and minor one is $BaTi_5O_{11}$ (BT_5, JCPDS 35-0805). The intensities of BT_5 peaks increase while those of BT_4 decrease from sample X1 to X3.

After calcining at 900 °C for 4 h, the main phase of the samples shown in Fig. 3 are still BT_4 and BT_5, while the relative amount of BT_5 gets more and more from sample X1 to X3, since the (0 4 1) peak of BT_5 becomes stronger and stronger.

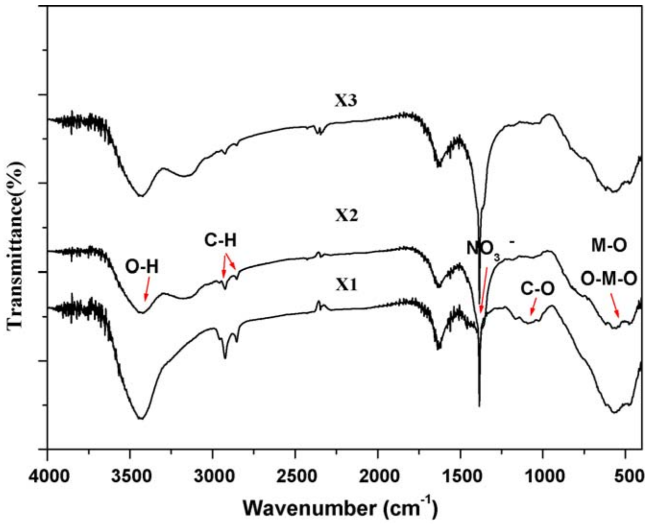

Fig. 1. FT-IR spectra of the combusted product of precursor solution.

Table 2
Element analysis of combusted products and corresponding BT_5/BT_4 ratio after calcinations.

Sample no.	Carbon%	BT_5/BT_4
X1	4.481	0.104
X2	1.512	0.311
X3	1.159	0.371

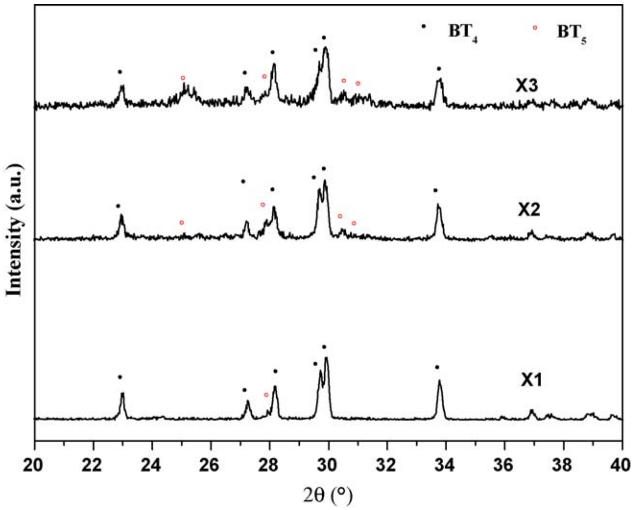

Fig. 2. XRD patterns of the combusted products of different precursor solutions.

The XRD patterns of the ceramics sintered at 1300 °C are shown in Fig. 4. It shows that main phase of the ceramic samples is B_2T_9, but minor BT_4 phase can still be found in sample X1 and X2. However, the phase in X3 is pure B_2T_9.

To study the effect of combustion on microstructure, the as-burnt product of sample X1 was characterized by TEM, and the image is shown in Fig. 5, in which two distinct different local parts can be resolved: part I-bulk grains (about 40–50 nm) and part II-nanoparticles (about 5–10 nm). According to the electron diffraction (ED) pattern and energy dispersive spectra (EDX), part I is crystalline and part II is amorphous in a higher carbon

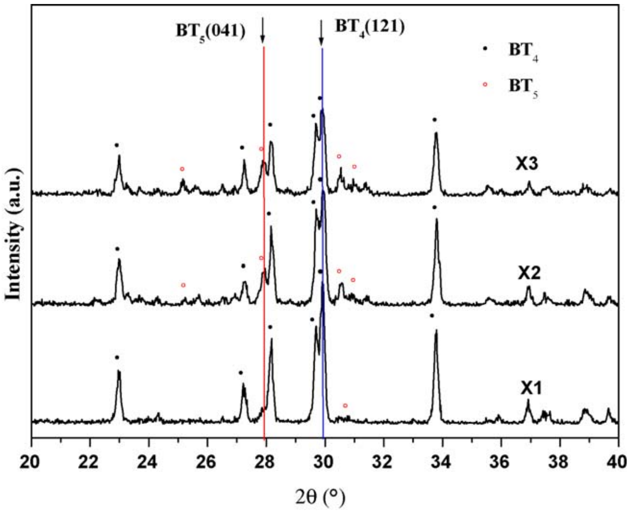

Fig. 3. XRD patterns of the calcined products of different precursor solutions.

content ambient. Further EDX analysis shows that the ratio of Ti/Ba in part I is 3.8, while 5.1 in part II (Table 3), that indicates the formation of Ti-rich amorphous component during the incomplete oxidation in X1.

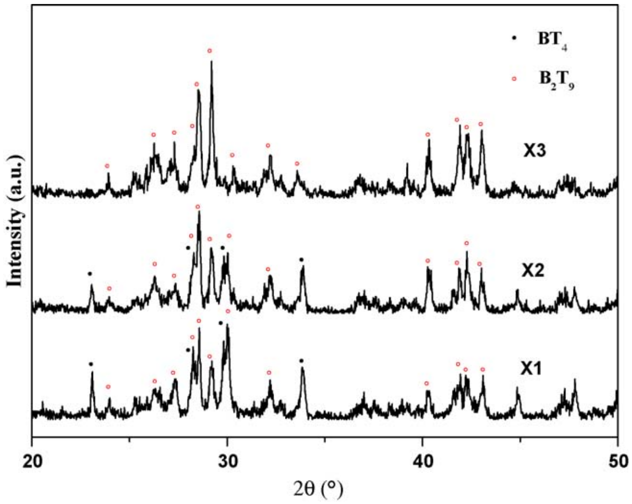

Fig. 4. XRD patterns of sintered ceramics at 1300 °C.

4. Discussion

According to Figs. 1–3, it is suggested that different combustion completeness leads to different product, especially

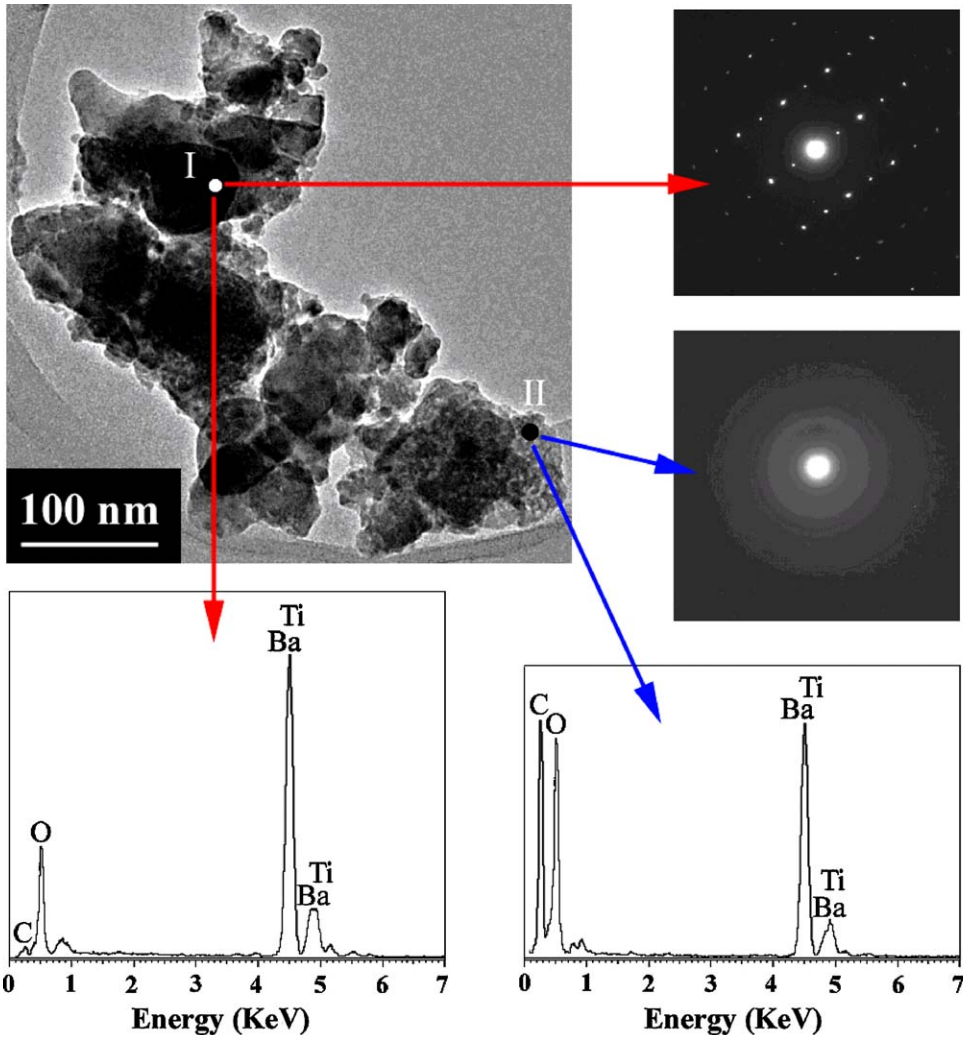

Fig. 5. TEM micrograph, electron diffraction diagram and energy dispersive spectrum of combusted products (X1).

Table 3
Element analysis comparison between part I and part II.

Element	Part I (Atomic%)	Part II (Atomic%)
C	5.60	53.04
Ti	43.16	12.38
Ba	11.41	2.42

affects the formation of the intermediate phase after calcining. Complete combustion facilitates the formation of BT_5 in the product before and after calcining. And high ratio of BT_5/BT_4 in calcined product favors the formation of B_2T_9 after sintering according Figs. 3 and 4, which corresponds to some early research [20,24].

In the combustion process, citric acid simultaneously has two actions: complexation and oxidation. The complexation makes metal ions in the solution dispersed uniformly in an interconnected gel network, and the oxidation causes a rapid temperature increase and results in nanocrystalline phase. The incomplete oxidation of citric acid will also influence the behavior of ions bonded to it. In the solution condition of pH ~6.0, $C_6H_5O_7{}^{3-}$ is the pre-dominant species, which can interact more strongly with Ba^{2+} and TiO^{2+} to form stable complexes $Ba(C_6H_5O_7)^-$ and $TiO(C_6H_5O_7)^-$ as the following [8,25]:

$$TiO^{2+} + C_6H_5O_7{}^{3-} = TiO(C_6H_5O_7)^- \quad \beta = 11.90$$

$$Ba^{2+} + C_6H_5O_7{}^{3-} = Ba(C_6H_5O_7)^- \quad \beta = 3.0$$

During the combustion process, the solution began to concentrate with the temperature increasing, and the organic network steadily forms due to the complexing between metal and organic substance. When the solution further concentrates to a certain stage, the network starts to break down into smaller organic moieties, some of which do not have any metal ions are volatilized. When the combustion takes place, the bondings between metal and organics in the network are broken, and the organics of large amount are oxidized, resulting in the crystallization of barium titanate (Fig. 5, part I). However, if the oxidation is incomplete, the residual organic component will wrap the metal ions, leading to an inhomogeneous dispersion of metal ions (Fig. 5, part II), which is unfavorable to the formation of the intermediate phase and final ceramics phase [12]. On the other hand, the stability coefficients, β, in above two complex equations are different, and the bonding between Ti and organic substance is stronger. If an incomplete combustion occurs, more residual organics surrounding Ti atoms will remain, and the Ti/Ba ratio in these locations will be higher as shown in part II than those in part I (Fig. 5). The inhomogenous system arises from the incomplete combustion (such as part II in Fig. 5) will hamper the BT_5 formation as an intermediate phase. As shown in Table 2, it is observed that the residual C in combusted product, as a symbol of incomplete combustion, is inversely proportional to BT_5/BT_4 ratio of intermediate phase. Here, the ratios are obtained from the intensity comparison between BT_5 (0 4 1) peaks and BT_4 (1 2 1) peaks in Fig. 3. It proves that the combustion extent has some tight connection with the intermediate phase formation, especially the formation of BT_5. And this result coincides with the TEM and EDX results very well. In Fig. 6, the high resolution XRD patterns of the calcined powder (Sample X1) give a further evidence of such inhomogeneity: minor TiO_2 phase (rutile, JCPDS 21-1276) is identified, which means impure phase is prone to occur in the calcining process under inhomogenous system from incomplete combustion.

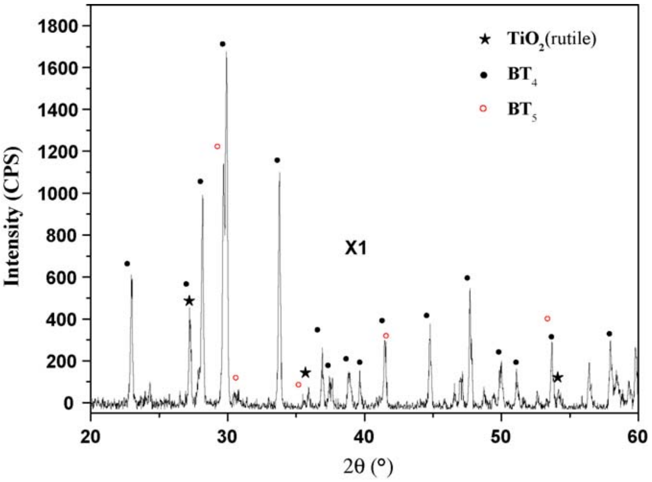

Fig. 6. The fine-analysis of calcined products XRD patterns.

Besides inhomogeneity, incomplete combustion has some other direct effects on crystallization: first, residual carbon oxidation in burnt product leads to crystals grown non-uniformity during the calcining process; second, extra steric hindrance is also imposed to the crystallization. Both reasons will also affect intermediate phase formation, finally hamper complete crystallization of B_2T_9.

5. Conclusions

$Ba_2Ti_9O_{20}$ powders and ceramics were prepared by the solution combustion method. The formation process is suggested to be 2 steps: firstly, intermediate BT_4 and BT_5 phase are formed; secondly, they further react to form B_2T_9 ($Ba_2Ti_9O_{20}$). During the combustion process, incomplete combustion shows negative effect in the whole CSC process: a large residual carbon increases the composition inhomogeneity of the combustion product, and brings other direct effects on crystallization during the calcined process, such as carbon oxidation, extra steric hindrance, etc. The addition of AN helps to avoid the happening of incomplete combustion and reduce these effects, thus promotes the formation of high purity B_2T_9 phase.

References

[1] H.M. O'Bryan, J. Thomson, J.K. Plourde, D.F. Linn, A new BaO–TiO_2 compound with temperature-stable high permittivity and low microwave loss, Journal of the American Ceramic Society 57 (10) (1974) 450–453.

[2] J.K. Plourde, D.F. Linn, H.M. O'Bryan, J. Thomson, $Ba_2Ti_9O_{20}$ as a microwave dielectric resonator, Journal of the American Ceramic Society 58 (9–10) (1975) 418–420.

[3] A. Feteira, D.C. Sinclair, I.M. Reaney, Y. Somiya, M.T. Lanagan, $BaTiO_3$-based ceramics for tunable microwave applications, Journal of the American Ceramic Society 87 (6) (2004) 1082–1087.

[4] C. Pithan, D. Hennings, R. Waser, Progress in the synthesis of nanocrystalline $BaTiO_3$ powders for MLCC, International Journal of Applied Ceramic Technology 2 (1) (2005) 1–14.

[5] X.R. Xing, J.X. Deng, J. Chen, G..R. Liu, Phase evolution of barium titanate from alkoxide gel-derived precursor, Journal of Alloys and Compounds 384 (2004) 312–317.

[6] A.V. Komarov, I.P. Parkin, New routes in the self-propagating high-temperature syntheses of barium titanium oxide, Polyhedron 15 (8) (1996) 1349–1353.

[7] W. Li, N. Wang, W.J. Wu, Y.L. Wang, M.Y. Zhao, Synthesis of $Ba_2Ti_9O_{20}$ powder via precipitation—mixing route, Materials Letters 59 (2005) 162–165.

[8] Y.B. Xu, X. Yuan, G.H. Huang, H. Long, Polymeric precursor synthesis of $Ba_2Ti_9O_{20}$, Materials Chemistry and Physics 90 (2005) 333–338.

[9] M.B. Park, N.H. Cho, C.D. Kim, S.K. Lee, Phase transition and physical characteristics of nanograined $BaTiO_3$ ceramics synthesized from surface-coated nanopowders, Journal of the American Ceramic Society 87 (3) (2004) 510–512.

[10] W.A. Sun, J.Q. Li, W. Liu, C.H. Li, Preparation of fine tetragonal barium titanate powder by a microwave—hydrothermal process, Journal of the American Ceramic Society 89 (1) (2006) 118–123.

[11] D.L. West, D.A. Payne, Preparation of $0.95Bi_{1/2}Na_{1/2}TiO_3{\cdot}0.05BaTiO_3$ ceramics by an aqueous citrate-gel route, Journal of the American Ceramic Society 86 (1) (2003) 192–194.

[12] A.G. Merzhanov, in: z.A. Munir, J.B. Holt (Eds.), Combustion and Plasma Synthesis of High-Temperature Synthesis: Twenty Years of Search and Findings, VCH, New York, 1990, p. 1.

[13] H.C. Yi, J.J. Moore, Review of self-propagating high-temperature synthesis (SHS) of powder-compacted materials, Journal of Materials Science 25 (1990) 1159.

[14] J.B. Holt, in: S.R. Lampman, M.S. Woods, T.B. Zorc (Eds.), Engineered Materials Handbook: Self-Propagating, High-Temperature Synthesis, vol. 4, Ceramics and Glasses, ASM International, Materials Park, OH, 1991, 227 pp.

[15] H.W. Wang, M.R. Chung, Formation of $Ba_2Ti_9O_{20}$ ceramics from EDTA-gel-derived powders, Materials Chemistry and Physics 77 (2002) 853–859.

[16] T.V. Anuradha, S. Ranganathan, Tanu Mimani, K.C. Patil, Combustion synthesis of nanostructured barium titanate, Scripta Materialia 44 (2001) 2237–2241.

[17] Z.M. Zhong, P.K. Gallagher, Combustion synthesis for $BaTi_4O_9$ and $Pb_xBa_{1-x}Ti_4O_9$, Journal of Materials Research 11 (1996) 162–168.

[18] Y.S. Zhang, G.C. Stangle, Preparation of fine multicomponent oxide ceramic powder by a combustion synthesis process, Journal of Materials Research 9 (1994) 1997–2004.

[19] L.J. Zhou, W.J. Weng, P.Y. Du, G. Shen, G.R. Han, Citrate solution combustion derived $Ba_2Ti_9O_{20}$ ceramics, Journal of the European Ceramic Society 26 (2006) 1995–1998.

[20] H.C. Lu, E. burkhart, G.L. Schrader, Sol–gel process for the preparation of $Ba_2Ti_9O_{20}$ and $BaTi_5O_{11}$, Journal of the American Ceramic Society 74 (5) (1991) 968–972.

[21] Z.M. Zhong, P.K. Gallagher, Combustion synthesis and characterization of $BaTiO_3$, Journal of Materials Research 10 (1995) 945–952.

[22] J. Poth, R. Haberkon, H.P. Beck, Combustion-synthesis of $SrTiO_3$. Part I. Synthesis and properties of the ignition products, Journal of the European Ceramic Society 20 (2000) 707–713.

[23] S.R. Jain, K.C. Adiga, V.R. Pai Verneker, A new approach to thermochemical calculations of condensed fuel-oxidant mixtures, Combustion and Flame 40 (1981) 71–79.

[24] J.M. Wu, H.W. Wang, Factors affecting the formation of $Ba_2Ti_9O_{20}$, Journal of the American Ceramic Society 71 (1988) 869–875.

[25] A. Ringbom, Complexation in Analytical Chemistry, Interscience, 1963 .